# Phase Front Instability in Periodically Forced Oscillatory Systems

Christian Elphick
*Centro de Fisica No Lineal y Sistemas Complejos de Santiago, Casilla 17122, Santiago, Chile*

Aric Hagberg*
*Theoretical Division and Center for Nonlinear Studies, MSB284, Los Alamos National Laboratory, Los Alamos, New Mexico 87545*

Ehud Meron†
*The Jacob Blaustein Institute for Desert Research and the Physics Department, Ben-Gurion University, Sede Boker Campus 84990, Israel*
(Received 8 January 1998)

Multiplicity of phase states within frequency locked bands in periodically forced oscillatory systems may give rise to front structures separating states with different phases. A new front instability is found within bands where $\omega_{\text{forcing}}/\omega_{\text{system}} = 2n$ $(n > 1)$. Stationary fronts shifting the oscillation phase by $\pi$ lose stability below a critical forcing strength and decompose into $n$ traveling fronts each shifting the phase by $\pi/n$. The instability designates a transition from stationary two-phase patterns to traveling $n$-phase patterns. [S0031-9007(98)06256-5]

PACS numbers: 82.40.Ck, 05.45.+b, 47.20.Ma, 82.20.Mj

Periodic forcing of a single oscillator can lead to rich dynamics including quasiperiodic oscillations, frequency-locked bands ordered through the Farey construction, and low-dimensional chaos [1–4]. A typical feature of a periodically forced oscillatory system is the multiplicity of phase states within a given frequency-locked band [5]. This feature becomes particularly significant in spatially extended systems where phase fronts separating different phase states may appear. The simplest situation arises in a system that is forced at twice the natural oscillation frequency (hereafter the 2:1 band). A phase front (kink) connecting two uniform states whose phases of oscillations differ by $\pi$ then exists (hereafter a "$\pi$ front"). The stability properties of this type of front are well studied [6–9]. As the strength of forcing is decreased a stationary front loses stability to a pair of counter-propagating fronts through a pitchfork bifurcation. The instability, known also as the nonequilibrium Ising-Bloch bifurcation [6,10], is responsible for the destabilization of standing waves and the onset of traveling wave phenomena including spiral waves.

The low resonance bands, 2:1 and 3:1, have been studied both theoretically [5–8,11,12] and experimentally [13]. All phase-front solutions in these bands shift the oscillation phase by the same angle (in absolute value): $\pi$ in the 2:1 band and $2\pi/3$ in the 3:1 band. At higher resonance bands phase fronts that shift the phase by different angles may coexist; for example, $\pi$ fronts and $\pi/2$ fronts in the 4:1 band. In this Letter we report on a new front instability: Upon decreasing the forcing strength a $\pi$ front within the $2n$:1 band $(n > 1)$ loses stability and decomposes into $n$ interacting $\pi/n$ fronts. We analyze in detail the 4:1 resonance case and bring numerical evidence for the existence of this type of instability in higher resonances.

We consider an extended system that is close to a Hopf bifurcation and externally forced with a frequency about 4 times larger than the Hopf frequency. The amplitude of oscillations satisfies the parametrically forced complex Ginzburg-Landau (CGL) equation [14,15]

$$A_t = (\mu + i\nu)A + (1 + i\alpha)A_{xx} - (1 - i\beta)|A|^2A + \gamma_4 A^{*3}, \tag{1}$$

where the subscripts $t$ and $x$ denote partial derivatives with respect to time and space, $A(x,t)$ is a complex field, and $\nu$, $\alpha$, $\beta$, and $\gamma_4$ are real parameters. We first consider the gradient version of Eq. (1) by setting $\nu = \alpha = \beta = 0$ and then rescale time, space, and the amplitude $A$ by $\mu$, $\sqrt{\mu/2}$, and $1/\sqrt{\mu}$, respectively. Keeping the same notations for the scaled quantities the gradient version takes the form

$$A_t = A + \frac{1}{2}A_{xx} - |A|^2A + \gamma_4 A^{*3}. \tag{2}$$

For $0 < \gamma_4 < 1$ Eq. (2) has four stable phase states: $A_{\pm 1} = \pm\lambda$ and $A_{\pm i} = \pm i\lambda$, where $\lambda = 1/\sqrt{1 - \gamma_4}$. Front solutions connecting pairs of these states divide into two groups: $\pi$ fronts connecting states with a phase shift of $\pi$

$$A_{-1\to+1} = A_{+1}\tanh x\,, \tag{3}$$

$$A_{-i\to+i} = A_{+i}\tanh x\,, \tag{4}$$

and $\pi/2$ fronts connecting states with a phase shift of $\pi/2$ [see Fig. 2(a)]. When $\gamma_4 = 1/3$ the $\pi/2$ fronts are given

  

by

$$A_{+1\to+i} = \frac{1}{2}\sqrt{\frac{3}{2}}[1 + i - (1 - i)\tanh x],$$

$$A_{-i\to+1} = \frac{1}{2}\sqrt{\frac{3}{2}}[1 - i + (1 + i)\tanh x], \quad (5)$$

$A_{-1\to-i} = -A_{+1\to+i}$ and $A_{+i\to-1} = -A_{-i\to+1}$. Additional front solutions follow from the invariance of Eq. (2) under reflection, $x \to -x$. For example, the symmetric counterparts of $A_{+i\to+1}(x)$ and $A_{+1\to-i}(x)$ are $A_{+1\to+i}(x) = A_{+i\to+1}(-x)$ and $A_{-i\to+1}(x) = A_{+1\to-i}(-x)$.

Stability analysis of the $\pi$ fronts (3) and (4) shows that they are stable for $\gamma_4 > 1/3$. To study the instability at $\gamma_4 = 1/3$ we rewrite Eq. (2) in terms of $U = \mathrm{Re}(A) + \mathrm{Im}(A)$ and $V = \mathrm{Re}(A) - \mathrm{Im}(A)$:

$$U_t = U + \frac{1}{2}U_{xx} - \frac{2}{3}U^3 - \frac{d}{2}(U^2 - 3V^2)U,$$

$$V_t = V + \frac{1}{2}V_{xx} - \frac{2}{3}V^3 - \frac{d}{2}(V^2 - 3U^2)V, \quad (6)$$

where

$$d = \gamma_4 - 1/3.$$

At $d = 0$ the two equations decouple and assume the solutions $U = \sigma_1 A_0(x - x_1)$ and $V = \sigma_2 A_0(x - x_2)$, where $A_0 = \sqrt{\frac{3}{2}}\tanh x$, $\sigma_{1,2} = \pm 1$, and $x_1$ and $x_2$ are arbitrary constants. Consider now $d \neq 0$ but small. The coupling between $U$ and $V$ makes $x_1$ and $x_2$ slow dynamical variables and $U$ and $V$ can be written as

$$U = \sigma_1 A_0[x - x_1(t)] + u,$$

$$V = \sigma_2 A_0[x - x_2(t)] + v, \quad (7)$$

where $u$ and $v$ are corrections of order $d$. Inserting these forms in Eqs. (6) we obtain

$$\mathcal{H}_1 u = \sigma_1 \dot{x}_1 A_0'(x - x_1) - \frac{1}{2}d\sigma_1[A_0^2(x - x_1) - 3A_0^2(x - x_2)]A_0(x - x_1),$$

where $\mathcal{H}_1 = -1 - \frac{1}{2}\frac{\partial^2}{\partial x^2} + 2A_0^2(x - x_1)$. A similar equation is obtained for $v$ with the indices 1 and 2 interchanged. Solvability conditions lead to the equation

$$\dot{x}_1 = -\frac{27}{16}d\int_{-\infty}^{\infty} dx \times \tanh(x - x_1)\,\mathrm{sech}^2(x - x_1)\tanh^2(x - x_2), \quad (8)$$

and to a similar equation for $x_2$ with the indices 1 and 2 interchanged. Defining a translational degree of freedom $\zeta = \frac{1}{2}(x_1 + x_2)$ and an order parameter $\chi = \frac{1}{2}(x_2 - x_1)$, we obtain from (8)

$$\dot{\zeta} = 0, \qquad \dot{\chi} = -\frac{27}{16}dJ(\chi), \quad (9)$$

where

$$J(\chi) = I(a) = 6(a^{-1} - a^{-3}) + (1 - 3a^{-2})G(a),$$

$$G(a) = (1 - a^{-2})\ln\left(\frac{1 + a}{1 - a}\right),$$

and $a = \tanh 2\chi$. Note that Eqs. (9) are valid to *all* orders in $\chi$ and to linear order around $\gamma_4 = 1/3$.

Figure 1 shows the potential $\mathcal{V}(\chi) = \frac{27}{16}d\int^{\chi} J(z)dz$ associated with Eq. (9) for $d > 0$ ($\gamma_4 > 1/3$) and $d < 0$. There is only one extremum point, $\chi = 0$, of $\mathcal{V}$. For $d > 0$ it is a minimum and $\chi$ converges to zero. For $d < 0$ it is a maximum and $\chi$ diverges to $\pm\infty$. To see how the $\chi$ dynamics affect the front solutions we rewrite the solution form (7) in terms of the amplitude $A$ and bring it to the form

$$A(x,t) = A_{-i\to+1}(x - x_1) + A_{+1\to+i}(x - x_2) - \lambda + R, \quad (10)$$

where $A_{-i\to+1}$ and $A_{+1\to+i}$ are given in Eqs. (5), $R$ is a correction term of order $d$ [related to $u$ and $v$ in Eqs. (7)] and for concreteness we chose $\sigma_1 = -\sigma_2 = 1$. Equation (10) describes two interacting $\pi/2$ fronts centered at $x_1$ and $x_2$. When $d > 0$ $|\chi|$ decreases in time and the two $\pi/2$ fronts attract. As $\chi \to 0$ (or $x_2 \to x_1$) the two $\pi/2$ fronts collapse into a single $\pi$ front, $A(x,t) = A_{-i\to+i}(x - x_1) + R$, given by Eq. (4). When $d < 0$ $|\chi|$ increases in time and the two $\pi/2$ fronts repel. Perturbing the unstable $\chi = 0$ solution, the single $\pi$ front decomposes into a pair of $\pi/2$ fronts. Figure 2(a) shows phase portraits of the $\pi$ and $\pi/2$ fronts (dashed lines) and the time evolution of an unstable $\pi$ front for $d < 0$ (solid lines) obtained by numerical integration of Eq. (2). The approach of the phase portrait to the fixed point $A_{+i}$ on the $\mathrm{Im}(A)$ axis describes the decomposition into

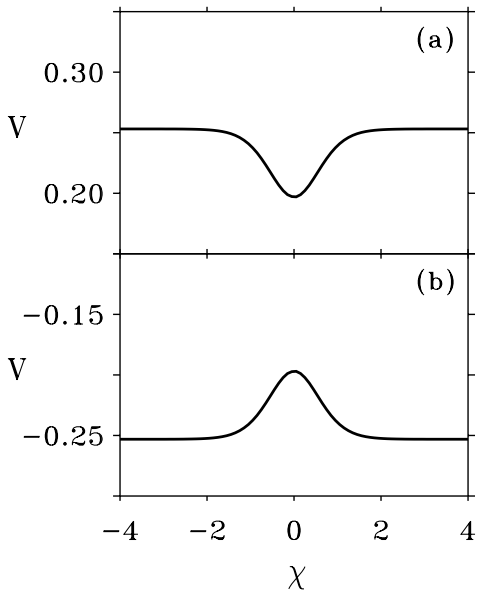


FIG. 1. The potential $\mathcal{V}(\chi)$. (a) For $d > 0$ the extremum at $\chi = 0$ is a minimum and $\chi$ converges to 0. (b) For $d < 0$ the extremum is a maximum and $\chi$ diverges to $\pm\infty$.

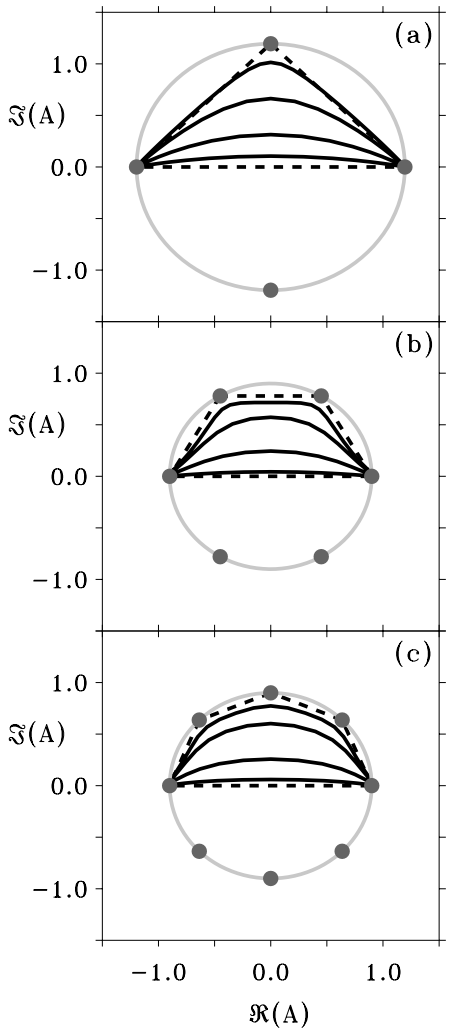


FIG. 2. Decomposition of $\pi$ fronts into $\pi/n$ fronts within $2n$:1 bands for (a) $n = 2$, (b) $n = 3$, and (c) $n = 4$. The dots are the uniform phase states along the circle of constant amplitude $|A|$. The $\pi$ fronts are the dashed lines connecting the states $A_{+1}$ and $A_{-1}$ on the Re($A$) axes. The $\pi/n$ fronts are the dashed lines connecting the adjacent points along the circle. The time evolution of the front decomposition obtained by numerical integration of Eq. (12) is shown as the series of solid lines. Parameters: all undetermined coefficients in Eq. (12) were set to zero except as indicated below. (a) $\gamma_4 = 0.3$, $\mu_4 = -1.0$; (b) $\gamma_6 = 0.9$, $\mu_4 = -1.0$, $\mu_6 = -1.0$; (c) $\gamma_8 = 0.75$, $\mu_4 = -0.5$, $\mu_6 = -0.5$, $\mu_8 = -1.0$.

a pair of $\pi/2$ fronts. This behavior persists *arbitrarily close* to $d = 0$ and is related to the absence of minima in the potential $\mathcal{V}(\chi)$ for $d < 0$ [see Fig. 1(b)]. At $d = 0$ there exists a continuous family of stationary solutions describing frozen (noninteracting) pairs of $\pi/2$ fronts with arbitrary separations $x_2 - x_1$. This solution family spans the whole phase space inside the dashed triangle in Fig. 2(a). Because of the parity breaking symmetry $\chi \to -\chi$ each $\pi$ front may decompose into one of two pairs of $\pi/2$ fronts with phase portraits approaching the fixed points $A_{+i}$ and $A_{-i}$.

We extended the derivation of Eqs. (9) to the nongradient equation (1), treating the constants $\nu$, $\alpha$, $\beta$ as small parameters. The $\chi$ equation remains unchanged. The $\zeta$ equation takes the form

$$\frac{\sigma_2}{\sigma_1}\,\dot{\zeta} = \nu F_\nu(\chi) + \alpha F_\alpha(\chi) + \beta F_\beta(\chi), \qquad (11)$$

where

$$F_\nu = -\frac{3}{4}\,G(a) - \frac{3}{2}\,a^{-1},$$

$$F_\alpha = \frac{3}{4}\,I(a),$$

$$F_\beta = 3a^{-1}\left(1 - \frac{3}{2}\,a^{-2}\right) - \frac{9}{4}\,a^{-2}G(a).$$

Notice that $F_\nu$, $F_\alpha$, and $F_\beta$ are odd functions of $\chi$ and do not vanish when $d = 0$. When $|\chi| \to \infty$ the right hand side of (11) converges to $\frac{3}{2}(\nu + \beta)$, the speed of a $\pi/2$ front solution of Eq. (1). The $\chi = 0$ solution (representing a $\pi$ front) remains stationary ($\dot{\zeta} = 0$) in the nongradient case as well. At $\gamma_4 = 1/3$ ($d = 0$) it loses stability and decomposes into a pair of $\pi/2$ fronts which approach the asymptotic speed $\frac{3}{2}(\nu + \beta)$. Depending on the initial sign of $\chi$ the pair may propagate to the left or to the right.

This behavior is different from that near the nonequilibrium Ising-Bloch front bifurcation within the 2:1 band. In that case, a stationary Ising front loses stability to a pair of counter-propagating Bloch fronts in a pitchfork bifurcation. Associated with the bifurcation is a transition from a single-well potential (Ising front) to a double-well potential (pair of Bloch fronts). A comparison with the potentials in Fig. 1 shows the essential difference between the two front instabilities. In the 2:1 band the Bloch fronts approach the Ising front and coincide with it as the distance to the bifurcation point diminishes to zero. In the 4:1 band, on the other hand, the asymptotic solutions just below $\gamma_4 = 1/3$ (the $\pi/2$-front pairs as $|\chi| \to \infty$) are not smooth continuations of the stationary $\pi$ front (the $\chi = 0$ solution) at $\gamma_4 = 1/3$. In particular their speed remains finite [$\frac{3}{2}(\nu + \beta)$] as $\gamma_4$ approaches $1/3$ from below. At $\gamma_4 = 1/3$, a whole family of propagating solutions appears with speeds ranging continuously from $\frac{3}{2}(\nu + \beta)$ to zero (pertaining to $\pi/2$-front pairs separated by distances ranging from infinity to zero).

The instability of $\pi$ fronts at $\gamma_4 = 1/3$ ($d = 0$) determines the structure of stable periodic patterns below and above the instability. In the range $\gamma_4 > 1/3$ *two-phase* patterns, involving domains separated by $\pi$ fronts, prevail. Below $\gamma_4 = 1/3$ *four-phase* patterns dominate. Four-phase patterns are not stable for $\gamma_4 > 1/3$ despite the stability of the $\pi/2$ fronts because of the attractive interactions among these fronts. In the gradient case [Eq. (2)] all solutions are stationary. In the nongradient case [Eq. (1)] the two-phase patterns are stationary while the four-phase patterns propagate. Figure 3(a) shows a

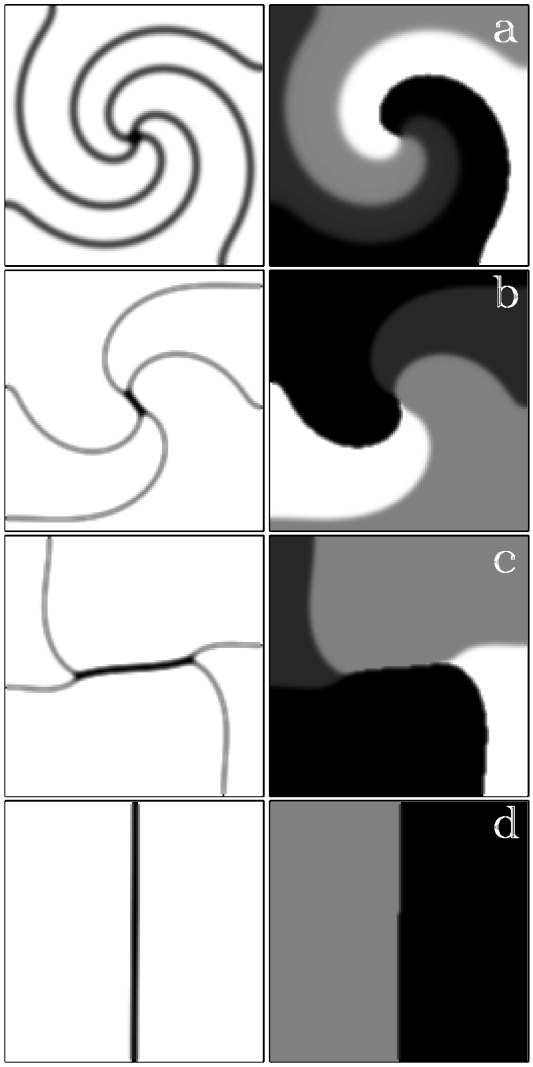


FIG. 3. Collapse of a rotating four-phase spiral wave into a stationary two-phase pattern. The left column is $|A|$ and the right column $\arg(A)$. (a) The initial four-phase spiral wave (computed with $\gamma_4 < 1/3$). (b) The spiral core, a four-point vertex, splits into two three-point vertices connected by a $\pi$ front. (c) A two-phase pattern develops as the three-point vertices further separate. (d) The final stationary two-phase pattern. Parameters: $\gamma_4 = 0.6, \nu = 0.1, x = [0, 64], y = [0, 64]$.

grey-scale map of a rotating four-phase spiral wave for $\gamma_4 < 1/3$. Figures 3(b), 3(c), and 3(d) show the collapse of this spiral wave into a stationary two-phase pattern as $\gamma_4$ is increased past $1/3$. The collapse begins at the spiral core where the $\pi/2$ front interactions are the strongest. As pairs of $\pi/2$ fronts attract and collapse into $\pi$ fronts, the core splits into two vertices that propagate away from each other leaving behind a two-phase pattern.

To test whether the instability of $\pi$ fronts exists at higher resonances we integrated numerically the higher order equation [16]

$$A_t = \frac{1}{2} A_{xx} + A + \mu_4 |A|^2 A + \mu_6 |A|^4 A + \mu_8 |A|^6 A + \gamma_4 A^{*3} + \gamma_6 A^{*5} + \gamma_8 A^{*7}. \quad (12)$$

Indeed $\pi$ fronts within the 6:1 and 8:1 bands become unstable as $\gamma_6$ and $\gamma_8$, respectively, are decreased below a critical value. Figure 2(b) shows the decomposition of a $\pi$ front into three $\pi/3$ fronts within the 6:1 band, and Fig. 2(c) shows the decomposition into four $\pi/4$ fronts within the 8:1 band. Our conjecture is that the instability is general, occurring within any $2n$:1 band ($n > 1$).

The phase front instability and the associated transition from stationary two-phase patterns to traveling four-phase patterns within the 4:1 band may be tested in experiments on the ruthenium-catalyzed Belousov-Zhabotinsky reaction subjected to periodic (in time) uniform illuminations [13].

We thank V. Petrov, H. L. Swinney, M. Clerc, R. Rojas, and E. Tirapegui for helpful discussions. This research was supported in part by Grant No. 95-00112 from the U.S.-Israel Binational Science Foundation (BSF). C. E. acknowledges the support of the Catedra Presidencial en Ciencias.

*Electronic address: aric@lanl.gov
†Electronic address: ehud@bgumail.bgu.ac.il

[1] M. J. Feigenbaum, L. P. Kadanoff, and S. J. Shenker, Physica (Amsterdam) **5D**, 370 (1982).
[2] D. Rand, S. Ostlund, J. Sethna, and E. Siggia, Physica (Amsterdam) **6D**, 303 (1984).
[3] M. H. Jensen, P. Bak, and T. Bohr, Phys. Rev. A **30**, 1960 (1984).
[4] J. Stavans, F. Heslot, and A. Libchaber, Phys. Rev. Lett. **55**, 596 (1985).
[5] D. Walgraef, *Spatio-Temporal Pattern Formation* (Springer-Verlag, New York, 1997).
[6] P. Coullet, J. Lega, B. Houchmanzadeh, and J. Lajzerowicz, Phys. Rev. Lett. **65**, 1352 (1990).
[7] P. Coullet and K. Emilsson, in *Instabilities and Nonequilibrium Structures V*, edited by E. Tirapegui and W. Zeller (Kluwer Academic Publishers, Dordrecht, 1996).
[8] B. A. Malomed and A. A. Nepomnyashcy, Europhys. Lett. **27**, 649 (1994).
[9] C. Elphick, A. Hagberg, E. Meron, and B. Malomed, Phys. Lett. A **230**, 33 (1997).
[10] A. Hagberg and E. Meron, Nonlinearity **7**, 805 (1994).
[11] P. Coullet and K. Emilsson, Physica (Amsterdam) **61D**, 119 (1992).
[12] L. Korzinov, M. I. Rabinovich, and L. S. Tsimring, Phys. Rev. A **46**, 7601 (1992).
[13] V. Petrov, Q. Ouyang, and H. L. Swinney, Nature (London) **388**, 655 (1997).
[14] J. M. Gambaudo, J. Differ. Equ. **57**, 172 (1985).
[15] C. Elphick, G. Iooss, and E. Tirapegui, Phys. Lett. A **120**, 459 (1987).
[16] No attempt has been made to include in Eq. (12) all resonant terms. We have included only terms that appeared necessary for demonstrating the phase front instability in the higher order 6:1 and 8:1 bands.